Chem. Senses 31: 795–806, 2006

doi:10.1093/chemse/bjl021
Advance Access publication August 16, 2006

A Comparison of Methods for Sniff Measurement Concurrent with Olfactory Tasks in Humans

Bradley N. Johnson[1,2], Cheryl Russell[3], Rehan M. Khan[2] and Noam Sobel[1,2,4]

[1]Joint Graduate Group in Bioengineering, UC Berkeley & UC San Francisco, [2]Helen Wills Neuroscience Institute, [3]Department of Bioengineering and [4]Department of Psychology, UC Berkeley

Correspondence to be sent to: Bradley N. Johnson, Helen Wills Neuroscience Institute, UC Berkeley, Berkeley, CA 94720, USA
e-mail: bnjohnso@socrates.berkeley.edu

Abstract

There is a growing appreciation for the role of sniffing in the formation of the olfactory percept. With this in mind, monitoring and measurement of sniffing is an important aspect of olfactory experiments. There are several methods for measuring human sniffs concurrent with odor delivery in olfactory experiments. Here, we set out to compare the temporal sensitivity and power of these different methods by applying them all simultaneously with an olfactory task. We discuss the advantages and disadvantages of each method and conclude in recommending the use of a nasal cannula linked to a pressure sensor whenever possible.

Key words: psychophysics, spirometer, respitrace, temperature, plethysmograph

Introduction

Researchers have long debated the proper management of sniffing during olfactory experiments. Whereas several early studies argued for the elimination of sniffing within olfactory experiments (Gamble 1899; Elsberg and Levy 1935), others have highlighted the importance of allowing near-natural olfactory behavior during olfactory tasks (Mainland and Sobel 2006). Indeed, the important role of sniffing in the formation of the olfactory percept has been highlighted in a recent series of reviews in this journal (Buonviso et al. 2006; Kepecs et al. 2006; Mainland and Sobel 2006; Schoenfeld and Cleland 2006). Considering the influence of sniffing on the resultant olfactory percept (Le Magnen 1945; Laing 1983) and on patterns of neural activity throughout the olfactory system (Tucker 1963; Sobel et al. 1998; Laurent 2002; Spors and Grinvald 2002; Kepecs et al. 2006), accurate measurement of sniff parameters is paramount. Although one can point to multiple sniff parameters of interest (Youngentob et al. 1987), the most important sniff measures are related to the temporal dynamics of the sniff and the resultant airflow volumetrics that deliver the odorant to the olfactory epithelium.

One can posit 2 reasons for measuring airflow in an olfaction study. The first reason is to know exactly how much odorant-laden air arrived at the sensory surface, namely, the olfactory epithelium. Experiments in cadavers (Paulsen 1882) and computational fluid dynamic models using computed tomography or magnetic resonance imaging generated from human nasal structures (Hahn et al. 1994; Keyhani et al. 1995; Zhao et al. 2004, 2006) have shown that the amount of air reaching the sensory epithelium is approximately 5–10% of the air entering the nostrils. However, considering individual variation in nasal structure, possibly enhanced by pathology, one cannot simply safely assume that 5–10% of what enters a nostril always reaches the epithelium. Due to this disparity, one would ideally measure the flow adjacent to the sensory epithelium. However, no such device for measuring airflow in the upper airway concurrent with an olfaction task is currently available for human studies.

A second reason for measuring sniffing during an olfaction task is to assure that sniffing behavior was held constant across different olfactory conditions or across repeated trials of the same condition. For example, one may be measuring the neural response to 2 different odors. In order to assure that variance in neural activity is reflecting the variance in odorants and not variance in sniffing behavior, one must assure that sniffing was constant. In this case, individual variability leading to differing epithelial exposure (e.g., polyps, septal deviation) across subjects is irrelevant because it remains constant within a subject across trials and conditions. It is this second reason for measuring sniffing that is addressed in this article.

Various methods have been employed in order to measure the external airflow sniff dynamics in humans. These

include 1) respiratory belts placed around the abdomen, chest, or both that measure respiratory sniff airflow–related expansion and contraction, 2) thermistors placed at the nares that measure the sniff airflow–related changes in temperature, 3) cannulas places at the nares and linked to pressure sensors that measure sniff airflow–related changes in relative pressure, and 4) pneumotachometers placed at the inlet of a nasal mask where they similarly measure sniff airflow–related changes in relative pressure. These methods are not all equally effective in measuring sniffing within an olfactory task. At times, the only information necessary is whether the subjects sniffed and when. For such gross information, it is likely that any of these measures is sufficient. However, some experiments call for more accurate measurements, and it is unknown which of these techniques effectively captures sniff dynamics.

For example, sniffs are odorant specific. Whereas intense and unpleasant odorants are sampled with moderate sniffs, mild and pleasant odorants are sampled with vigorous sniffs (Laing 1983; Warren et al. 1994; Sobel et al. 2001; Walker et al. 2001). This inverse relationship between sniff vigor and odorant magnitude is evident within as little as ~200 ms following sniff onset (Johnson et al. 2003) and is sufficiently stereotyped so as to serve as an olfactory clinical diagnostic tool (Frank et al. 2003). When studying such odorant-dependent sniffing, one would want increased temporal sensitivity in sniff measurement combined with minimal interference of the olfactory task. Here we set out to compare the sensitivity of different methods for sniff measurement in the context of odorant-specific sniffing. Subjects sniffed either an intense unpleasant odorant or a mild pleasant odorant concurrent with sniff measurement using all the 4 above-mentioned methods simultaneously.

Materials and methods

Subjects

Twenty-one college students (8 females), aged 18–23, participated in the experiment after giving informed consent to procedures that conformed to National Institutes of Health guidelines and were approved by the University of California, Berkeley, Committee on Protection of Human Subjects. Subjects were screened for no history of nasal trauma or neurological disease, no regular use of medication, and self-reported intact olfactory acuity.

Testing room

Testing was performed in a designated 9 × 11–ft room that was completely coated with stainless steel to prevent odor contamination. The room was equipped with high efficiency particulate air and carbon high-rate filtration to further minimize odorant contamination. Subjects were comfortably seated in a dental chair centered in the room. During experimentation, subjects were alone in the room, monitored via a one-way mirror window, and video monitor in the adjacent control room.

Sniff measurement

Subjects were fitted with plethysmograph belts (respitrace), nasal temperature sensors, nasal pressure sensors, and nasal mask pneumotachometer, allowing simultaneous recording of all measures (Figure 1).

Respitrace

We used 2 piezoelectric respiratory belt transducers (MLT1132, ADInstruments, Grand Junction, CO) for the respiratory plethysmograph recording. One belt was placed at the level of the abdomen, and the other was placed at the level of the chest. Each belt contains a piezoelectric element that responds to length changes, requires no driving circuitry, and connects directly to an instrumentation amplifier.

Temperature

We used 2 thermistors that were designed specifically for the measurement of nasal airflow–related changes in temperature (MLT415/A, ADInstruments). One thermistor was placed at the opening of each nostril. Each thermistor was

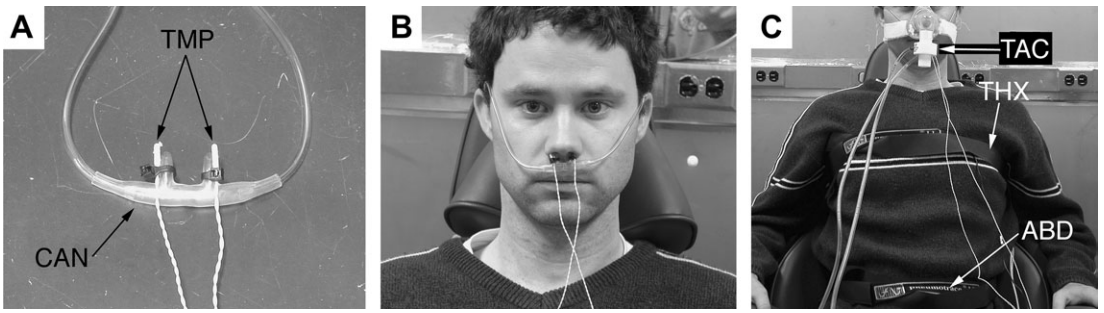

Figure 1 Subject setup. Panel **A** shows the cannula (CAN) that is attached to the piezoelectric pressure sensor (not shown) and the 2 thermistors (TMP). Small zip-ties are used to fasten the thermistors to each orifice of the cannula. Panel **B** shows the CAN and TMP apparatus attached to a subject. The remaining measurement devices are shown in panel **C**. The thoracic belt (THX) is secured below the arms, whereas the abdomen belt (ABD) is secure around the midsection at the level of the naval. The pneumotachometer flow head (TAC) is attached to the mask via a short flexible tube.

attached to a signal conditioner allowing resolution of 0.01 °C (Thermistor POD MC309, ADInstruments) and then to an instrumentation amplifier. Critically, when placing these sensors, we made sure that the sensing element was not in direct contact with the skin but rather suspended in the nostril orifice. Direct contact with the skin acts as a heat sink that significantly reduces sensitivity.

Pneumotachometer

We used a pneumotachometer (high-sensitivity flowmeter model #4719, Hans Rudolph, Inc., Kansas City, MO) that was attached in-line with the vent port of the nasal mask. The pneumotachometer differential pressure was measured and converted to a voltage signal using a spirometer (ML141, ADInstruments) that delivered the voltage to an instrumentation amplifier.

Pressure

We used a respiratory nasal cannula (#1600, Salter Labs, Avin, CA, http://www.salterlabs.com) attached to a small piezoelectric silicon device (30INCH-D-MV, AllSensors, http://www.allsensors.com) with adjacent signal conditioning circuitry (described in detail in Appendix) for the millivolt output from the transducer to an instrumentation amplifier. The pressure transducer was calibrated with a manometer to allow conversion from volts to millimeters of H_2O.

All measurements were simultaneously acquired and sampled at 1 kHz using an ADInstruments PowerLab 16SP instrumentation amplifier and Chart v5.0 software for digital recording. All channels were low-pass filtered (100 Hz) by the instrumentation amplifier.

Olfactometer

The olfactometer was based on previously described theoretical designs (Benignus and Prah 1980; Kobal 1985; Prah et al. 1995). All wetted parts of the olfactometer were made of stainless steel or Teflon. The olfactometer was driven by custom software written in LabVIEW (National Instruments, Austin, TX) that controlled 1) odorant identity, 2) odorant concentration, 3) gas flow rate, 4) flow temperature, 5) flow humidity, and 6) odorant delivery timing. Odorant identity was achieved by flowing a carrier gas, medical-grade breathing air, over undiluted liquid of the odorant placed in a specially designed stainless steel canister with 510-mm^2 surface area. The carrier gas pulled away the vapor of the evaporating liquid. Concentration range was accomplished by mixing clean and odorized air using electronic mass flow controllers (MFCs, M100B, MKS Instruments, Methuen, MA). At the olfactometer output, MFCs controlled a clean air line, an odorized air line, and 2 vacuum lines, all joining at a "railroad switch" under the subject's nose. Switching between odorant and no-odorant conditions was accomplished by activating a 3-way solenoid that pulled vacuum from only one of the 2 vacuum lines. This resulted in removal of either the odorized or the clean air from the railroad switch, allowing only the other air source to reach the nose. The outcome was a seamless shift between odorant and no-odorant conditions with no visual, auditory, tactile, humidity, or thermal cues as to the alteration. For more details on the construction and performance of the device used, see Johnson et al. (2003).

Odorants

Two odorants were used in the study, phenethyl alcohol (99%+, P1 360-6, Sigma-Aldrich, http://sigmaaldrich.com) and valeric acid (99%+, 129542, Sigma-Aldrich, http://sigmaaldrich.com). These odorants were chosen because they are commonly reported as pleasant (phenethyl alcohol) and unpleasant (valeric acid) (Doty 1975). We used 1 concentration of each odorant that corresponded to 100% of full maximum at 6 LPM over 8 ml of liquid odorant in the stainless steel canister. In this article, the phenethyl alcohol trials are identified PEA and the valeric acid trials as VAL. In addition to the PEA and VAL conditions, we used a third condition of 6 LPM clean air and identified it as AIR.

In order to estimate the absolute concentration of the stimuli used, we measured the depletion rate of liquid odorant as a function of carrier gas flow rate (Allison and Katz 1919; Johnston 1967). Odorant was loaded into the olfactometer after measuring the initial mass with an analytical balance (L-Series, 0.1 mg precision, Acculab, Bradford, MA). Odorized air at 6 LPM carrier gas flow rate was produced by the olfactometer for a 20- to 30-min period, after which the remaining mass was measured. The total volume of air was measured by integrating the flow measurement by the olfactometer. The mass loss was converted to moles (mass/molecular weight) and then to molar concentration (moles of odor vapor per million moles of carrier gas at 1 atm and 37 °C). The obtained values were then used to assess the diluted concentration for the flow rate used in this experiment. Based on these measurements, we estimated the final sniffed concentrations to be about 0.15 ppm for PEA and 0.23 ppm for VAL.

Experimental design

Each experiment contained 30 trials with a 45-s intertrial interval, 10 trials for each condition (VAL, PEA, and AIR). For each trial, the following digitized audio and visual command queue was given: "please prepare to sniff at the tone," "3," "2," "1," tone. At the tone, the subject took one sniff that contained PEA, VAL, or AIR delivered in a counter-balanced order. Following the sniff, the subject used a trackball to rate the odorant intensity and pleasantness on an on-screen visual analog scale. All experimental components, including task instructions, odorant delivery and triggering, and acquisition of both respiratory and perceptual data, were computer controlled and administered via digitized voice, thus preventing any unintentional experimenter-related cues or bias.

Data reduction

Odorant perceptual data

Perceptual responses were averaged across repeats of the same odorants within each subject, graphed, and tested for significant differences.

Sniff data

We first eliminated one thermistor trace and added one computed respitrace measure as follows: There is often a difference across nostrils in the rate of airflow (Principato and Ozenberger 1970; Hasegawa and Kern 1977). Because the thermistor reflects airflow-dependent changes in temperature, it provides increased signal from the nostril with greater airflow (indeed, sometimes one nostril had almost no sniff-related changes in temperature). Thus, we first selected for each subject the thermistor trace with greater signal and used only that for further analysis. In turn, we added the commonly used computed respitrace measure that is the weighted sum of 2 times thoracic and abdominal measures (Banzett et al. 1995).

Sniffing data was first converted from Chart binary files into ASCII text files that were then loaded into MATLAB 6.5 (Mathworks, Inc., Natick, MA). MATLAB was used for all subsequent analysis. Each data trace was then preprocessed in an identical way—data was low-pass filtered, third-order Butterworth Fc = 10 Hz, and then phase corrected to compensate for the temporal shift produced by the filter. All trials were then aligned in time, DC offset was removed, and then data was scaled to the maximum (minimum for temperature) value collected for that measure in that subject. Finally, for each trial, the data trace was truncated at 4000 ms.

To parameterize the time series data for statistical analysis, we calculated 3 summary variables: mean value, max value, and the integral (e.g., area under the curve). For each of these summary variables of each measurement technique, we calculated an *F*-statistic using a 1-way repeated measures analysis of variance (ANOVA). Additionally, we calculated the *F*-statistic versus time. We did this in 2 slightly different ways. In the first method, the input parameter to the ANOVA was the value from the time series at that particular time point. In essence, we created an ''instantaneous'' estimate of the *F*-statistic that was independent from prior ANOVAs in as much as the time series data are independent. In contrast, the second method calculated the *F*-statistic for successively longer time periods, where we used the integral within this growing time period as the measured parameter for the ANOVA. That is, each successive ANOVA computation was the same as the previous one, except that we added another 10 ms of data. This procedure created a ''running'' estimate of the *F*-statistic versus time that was dependent on all data back to time zero.

To compare the overall statistical sensitivity of each measure, we used bootstrapping (Efron and Tibshirani 1993) to create distributions of the *F*-statistic for the 3 summary variables (mean, max, and integral) for each measurement technique and then used these distributions to compare the various measurement techniques. The bootstrapping was done as follows. Within each subject and condition, we randomly selected 10 repeats (e.g., trials), allowing individual repeats to be selected more than once (e.g., random with replace). These 10 repeats were averaged and thus formed a ''resampled'' version of a particular subject's response to condition X. After resampling all subjects and the 3 conditions, we computed the 3 summary variables (mean, max, and integral) and then computed the *F*-statistic from these values. This technique allowed us to estimate the variance of the *F*-statistics determined from the original data.

Results

Data from 7 subjects was eliminated from the subsequent data analysis. One subject was excused because of technical problems (communication between the olfactometer and acquisition software) that could not be resolved during the allotted experiment time period, one subject was excused during the training period because they were uncooperative, three subjects were eliminated for missing more than 3 trials during the experiment, and two subjects were eliminated for failure of the nasal cannula measurement channel. The 2 nasal cannula failures reflected the various hardware (wire, cabling, tubing, etc) of one measurement interfering with the hardware of another measure. Typically, movement of the nasal mask or movement of the thermistor cable pulled out the nasal cannula. Because the simultaneous recording of all measures was critical for this study, subjects where any measure was eliminated were then completely eliminated from analysis. This left 16 subjects for further analysis. It is noteworthy that this attrition rate does not reflect a realistic attrition rate of the nasal cannula but rather is related to the specific design of this study where placement of one measure complicated the placement of another. In a typical olfaction study, one would use only one of these devices, and from our experience, when used alone, the attrition rate of these devices is negligible.

We conducted 4 separate analyses of our data. The first analysis was to determine the perceptual differences between the 3 stimulus conditions. In the second analysis, we assessed each techniques' ability to reveal odorant-specific sniffing. In the third analysis, we directly compared the signal-to-noise ratios for each measurement technique. Finally, in the fourth analysis, we examined the temporal response of each measurement technique.

Odorant perceptual data

We first examined the intensity and pleasantness responses to ensure that the chosen odorants were perceived differently. The group mean perceptual results shown in Figure 2 demonstrate that we successfully generated 2 very different

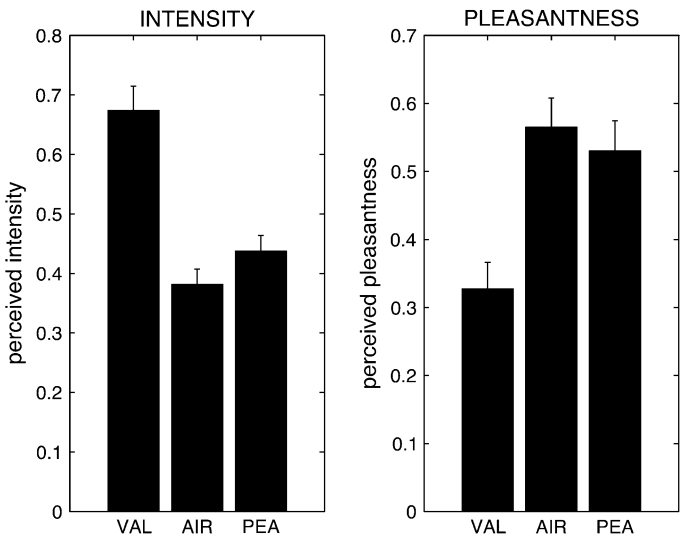

Figure 2 Perceptual results. Group mean estimates for intensity (left) and pleasantness (right) for the 3 conditions: valeric acid (VAL), clean air (AIR), and phenethyl alcohol (PEA). Errors bars are ±1 SE but are not representative of actual within-subject differences. There was a significant effect for condition on perceived intensity ($F(2, 30) = 38.9$, $P < 4.6 \times 10^{-9}$) and perceived pleasantness ($F(2, 30) = 22.27$, $P < 1.2 \times 10^{-6}$).

odorants. There was a significant effect of condition on perceived intensity ($F(2, 30) = 38.9$, $P < 4.6 \times 10^{-9}$) and perceived pleasantness ($F(2, 30) = 22.27$, $P < 1.2 \times 10^{-6}$). Post hoc analysis using multiple comparisons–corrected t-tests showed a significant intensity difference between AIR and VAL ($t(15) = -7.9371$, $P < 1 \times 10^{-6}$), PEA and AIR ($t(15) = 2.3245$, $P < 0.035$), and PEA and VAL ($t(15) = -5.6064$, $P < 1 \times 10^{-4}$) and a significant pleasantness difference for AIR and VAL ($t(15) = 5.2021$, $P < 1 \times 10^{-4}$) and PEA and VAL ($t(15) = 4.6485$, $P < 3 \times 10^{-4}$) but not for PEA and AIR ($t(15) = -1.6439$, $P = 0.121$). In summary, VAL differed from PEA in both intensity and pleasantness. See Table 1 for mean and variance estimates for the ratings of each condition.

It is important here to remind that if one were setting out to test which particular olfactory aspects most influence sniffing, the above olfactory perceptual space would be suboptimal in that it would be hard to dissociate whether odorant intensity or pleasantness influenced sniffing patterns. In this study, however, we set out to create 2 stimuli that differed in a manner that was sure to be accompanied by different sniffs, so that we could address our question of interest, namely, the sensitivity of different sniff measurement techniques.

Summary variables revealing odorant-induced changes in sniffing

To begin analyzing the sniffing data, we determined which technique showed differences between our 3 odorant conditions. We created the various summary variables (mean, max, integral) as detailed in Data Reduction and then calculated a 1-way repeated measures ANOVA to determine which summary variables were different between the 3 odorant conditions. The group mean time series and group mean summary variables for each measurement technique are shown in Figure 3. Overall, we found that every measure but one was able to discriminate odorant-induced sniffing changes to some degree. Only the thorax belt (and combo thorax + abdominal) showed no difference for any of the 3 summary variables (volume, mean, or max). However, the abdomen belt showed significant differences for mean ($F(2, 30) = 3.534$, $P < 0.042$). The pneumotachograph showed significant differences for volume ($F(2, 30) = 4.93$, $P < 0.014$) and mean ($F(2, 30) = 4.06$, $P < 0.023$). The nasal cannula showed significant differences for volume ($F(2, 30) = 8.18$, $P < 0.002$), max ($F(2, 30) = 4.38$, $P < 0.02$), and mean ($F(2, 30) = 7.36$, $P < 0.003$). The temperature sensor showed significant differences for volume ($F(2, 30) = 7.31$, $P < 0.003$), max ($F(2, 30) = 12.11$, $P < 0.0001$), and mean ($F(2, 30) = 8.88$, $P < 0.0009$). Post hoc analysis to determine individual condition differences consistently showed separation between VAL and AIR and less frequently between AIR and PEA or VAL and PEA. See Table 1 for mean and variance estimates for each summary variable.

Rank ordering of measurement signal-to-noise

We next set out to determine which measurement technique showed the greatest differences between the 3 odorant conditions. We used the F-statistic from the ANOVA as an estimate of each techniques' signal-to-noise ratio, that is, how sensitive it was to differences among the different sniff conditions.

The F-statistic for each summary variable is shown in Figure 4 and are the same F-statistics reported above (summary variables revealing odorant-induced changes in sniffing). The dotted line in Figure 4, at $F = 3.3158$, represents the critical value for an alpha = 0.05 level of significance. The bar graphs convey the picture that the spirometer, pressure, and temperature have a generally better signal-to-noise ratio than the respiratory band methods. In order to compare the measures statistically, we need to know the error distribution of the F-statistic in each condition. We used bootstrapping, a resampling procedure (Efron and Tibshirani 1993), to construct error distributions for the F-statistic in each condition.

For every bootstrap iteration, we obtained an estimated F-statistic for each of the 18 variables shown in Figure 4. These estimates allowed us to generate distributions for each of these 18 variables. We then calculated the standard deviation for each distribution and displayed them as the error bars in Figure 4. The means of these distributions generally agreed with, although were slightly less than, the F-statistics calculated from the actual data (e.g., that shown in Figure 4). These variance estimates allow for visual comparison of the 18 variables.

To statistically compare the 18 variables, we again used the bootstrap analysis. To determine if these differences in the

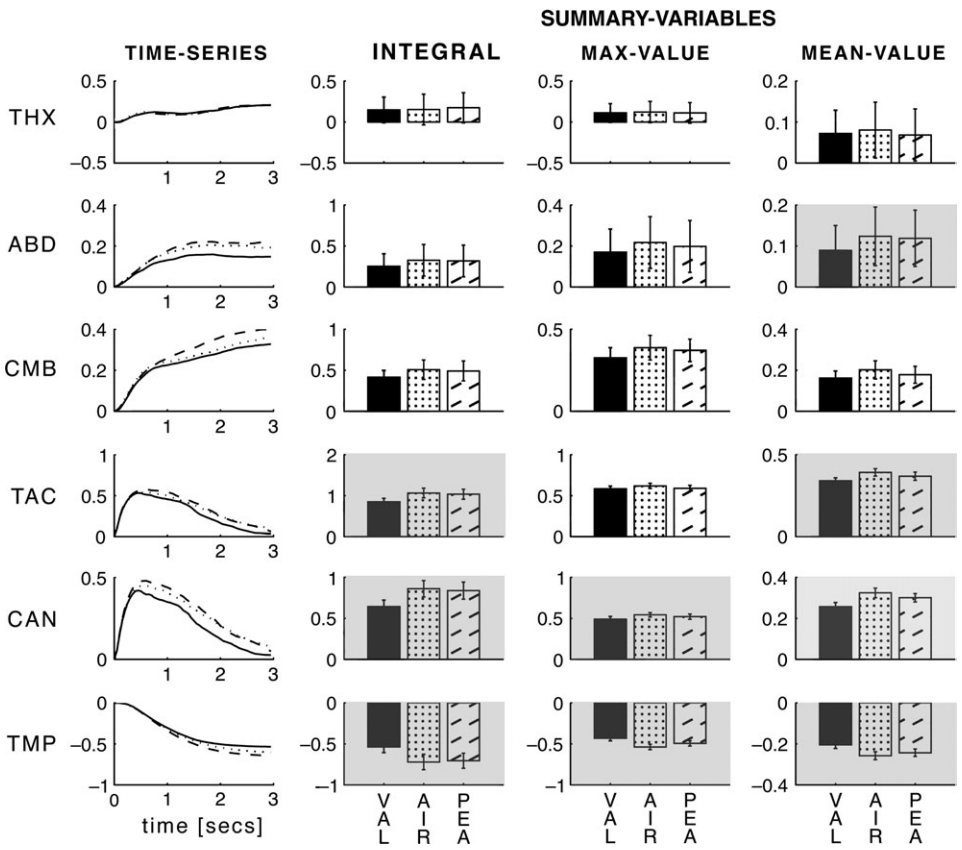

Figure 3 Group mean time series (left most panel) and group mean summary variables (right 3 panels) for each measurement technique. Solid lines and bars are for valeric acid (VAL), dotted lines and bars for clean air (AIR), and dashed lines and bars for phenethyl alcohol (PEA). The measurements are abbreviated: thorax belt (THX), abdomen belt (ABD), respitrace combination (CMB), pneumotachograph (TAC), nasal cannula (CAN), and temperature (TMP). The errors bars in the summary variable panels represent ±1 SE and represent the between-subject error and not the within-subject as tested by the ANOVA. Panels with a significant ANOVA ($P < 0.05$) are highlighted by the gray background shading.

F-statistic are significant, we pairwise compared the measurement techniques that were significant, abdomen belt (ABD), pneumotachograph (TAC), nasal cannula (CAN), and temperature (TMP), for each summary variable (volume, max, and mean) for each bootstrap iteration. That is, for each of the 1,000 iterations of the bootstrapping, we obtained a number that was the difference in *F*-statistic value for a particular summary variable between 2 measurements, for example, pneumotachograph and nasal cannula (TAC vs. CAN). If there were no difference between the *F* values produced by the measurement techniques, then the pairwise subtraction of the *F*-statistic values would yield a distribution centered around zero. That is, for every bootstrap iteration, there is an equal probability that the pairwise subtraction will fall above or below zero. Thus, we estimated the probability to observe only *N* samples above (or below) zero as *N*/500 or alpha = *N*/500. For the volume summary variable, we found significantly higher signal-to-noise (*F* value) for the TAC versus ABD ($P < 0.001$), for the CAN versus ABD ($P < 0.001$), and for the TMP versus ABD ($P < 0.004$) but not for CAN versus TAC ($P \sim 0.09$), TMP versus TAC ($P \sim 0.61$), or TMP versus CAN ($P \sim 0.58$). For the max value summary variable, we found significant differences for TMP versus ABD ($P < 0.02$) and TMP versus TAC ($P < 0.04$) but not for TAC versus ABD ($P \sim 0.77$), TAC versus ABD ($P \sim 0.77$), CAN versus ABD ($P \sim 0.27$), CAN versus TAC ($P \sim 0.20$), or TMP versus CAN ($P \sim 0.22$). Using the mean parameter, there was no significant difference between the measurement parameters.

Comparing temporal response of each measurement

In our last analysis, we examined the behavior of the *F*-statistic as a function of time (e.g., from sniff onset to the end of the sniff) to compare the temporal responses of the measurement techniques. To examine the behavior of the *F*-statistic over time, we plotted the instantaneous and running *F* value for our actual data (not the resampled bootstrap iterations) in Figure 5. There is a very small time window where the abdomen belt is significant (~1000 ms, $P < 0.05$); however, this separation is not sustained as in the other measurements. The spirometer is significant past ~500 ms (instantaneous) or ~1000 ms (running). The pressure is significant past ~400 ms (instantaneous) or ~600 ms (running).

Table 1 Consolidated data from ANOVA tests

		VAL	AIR	PEA	*F*	*P*	SD bootstrap
Perceived intensity rating		0.673 ± 0.042	0.382 ± 0.026	0.437 ± 0.027	38.9009	4.60×10^{-9}	N/A
Perceived pleasantness rating		0.327 ± 0.039	0.565 ± 0.043	0.530 ± 0.044	22.2698	1.20×10^{-6}	N/A
Thorax	Integral	0.147 ± 0.157	0.153 ± 0.187	0.173 ± 0.184	0.1126	0.8939	0.3696
Thorax	Max value	0.110 ± 0.113	0.122 ± 0.130	0.111 ± 0.126	0.0612	0.9408	0.3584
Thorax	Mean value	0.072 ± 0.057	0.080 ± 0.068	0.068 ± 0.064	0.2027	0.8176	0.38
Abdomen	Integral	0.250 ± 0.153	0.323 ± 0.191	0.312 ± 0.193	0.8112	0.4538	0.5832
Abdomen	Max value	0.170 ± 0.113	0.217 ± 0.126	0.197 ± 0.127	1.6662	0.206	0.9734
Abdomen	Mean value	0.089 ± 0.061	0.123 ± 0.071	0.118 ± 0.069	3.53	0.0419	1.561
Combo	Integral	0.412 ± 0.085	0.506 ± 0.118	0.491 ± 0.121	1.4131	0.2591	0.9741
Combo	Max value	0.325 ± 0.062	0.388 ± 0.075	0.371 ± 0.069	1.7482	0.1914	1.2377
Combo	Mean value	0.161 ± 0.035	0.202 ± 0.044	0.178 ± 0.041	2.006	0.1522	1.1469
Pneumotac	Integral	0.849 ± 0.086	1.063 ± 0.117	1.034 ± 0.123	4.9335	0.014	1.362
Pneumotac	Max value	0.581 ± 0.035	0.618 ± 0.032	0.589 ± 0.036	1.6461	0.2097	1.1594
Pneumotac	Mean value	0.340 ± 0.019	0.392 ± 0.022	0.368 ± 0.025	4.0558	0.0276	1.6895
Cannula	Integral	0.641 ± 0.081	0.860 ± 0.100	0.837 ± 0.105	8.1849	0.0015	2.0606
Cannula	Max value	0.488 ± 0.035	0.542 ± 0.027	0.521 ± 0.031	4.3826	0.0214	2.1415
Cannula	Mean value	0.256 ± 0.021	0.324 ± 0.023	0.300 ± 0.020	7.3643	0.0025	2.6243
Temperature	Integral	−0.538 ± 0.070	−0.722 ± 0.095	−0.706 ± 0.091	7.3139	0.0026	2.0964
Temperature	Max value	−0.431 ± 0.033	−0.538 ± 0.033	−0.494 ± 0.031	12.1081	0.0001	3.4898
Temperature	Mean value	−0.204 ± 0.018	0.258 ± 0.019	−0.243 ± 0.018	8.8795	0.0009	3.1173

The measurement technique and summary variables vary by row. The group mean value and standard error for each stimulus condition (e.g., valeric acid, air, and phenethyl alcohol) are shown in the respectively headed columns (e.g., VAL, AIR, and PEA). The *F* and *P* values for each test are shown in the associated columns (e.g., *F* and *P*). Finally, the standard deviation (SD) from the associated bootstrap distribution is shown in the right-most column (e.g., SD bootstrap). N/A = not applicable.

Finally, the temperature sensor did not reach significance until ~900 ms (instantaneous) or ~1100 ms (running).

These findings are consistent with the previous analysis using volume, max, and mean, but the added temporal sensitivity has allowed us to locate the obvious temporal performance differences between the spirometer, pressure, and temperature sensors. Overall, the temperature sensor had the highest *F*-statistic, provided it had access to the entire sniff. However, when temperature was examined for the first second, not only did it perform worse than the pressure sensor but also the *F*-statistic for the actual data did not produce an alpha < 0.05 until after ~1 s, whereas both the pressure and spirometer did so at around 500–600 ms (Figure 5).

Discussion

In this study, we sought to determine which of the most commonly used sniff-monitoring techniques are suitable for use in olfactory experiments. We were particularly interested in techniques that were sensitive enough to show odorant-related sniff modulation. We found that a thoracic respiratory belt did not provide information sufficient for dissociating odorant-specific sniffs. Furthermore, a commonly used computed combination of thoracic and abdominal respiratory belts was also not sufficiently sensitive. This information is important because often these very measures have been used to assure that sniffing was constant across different olfactory conditions within a study. Our results suggest that in the future other methods of measuring sniffing should be applied in order to substantiate such statements. In contrast, an abdominal respiratory belt, temperature sensors in the nostrils, and measures of sniff-induced pressure differences measured either in the nose by cannula or around the nose through nasal mask were all sufficiently sensitive. If one is interested in an overall odorant-dependent sniff difference, the rank ordering of these measurements from most to least powerful is as follows: temperature, nasal cannula (attached to pressure sensor), pneumotachometer flow head (attached to spirometer pressure sensor), and lastly abdominal belt.

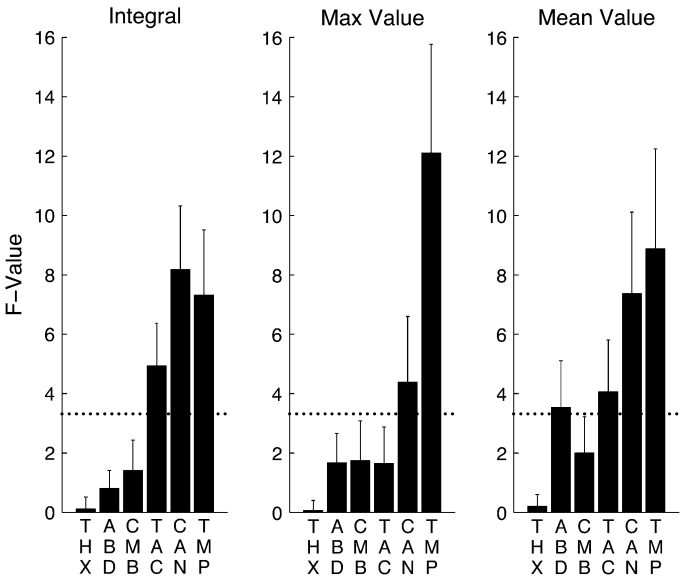

Figure 4 *F* values of the 1-way repeated measures ANOVAs on the actual data, for each summary parameter: integral (left), max value (middle), and mean value (right). The 6 measurement techniques are represented within each bar graph as follows: thoracic belt (THX), abdominal belt (ABD), combined belts (CMB), pneumotachograph (TAC), cannula (CAN), and temperature (TMP). The dotted line ($F = 3.3158$) is alpha = 0.05 (degrees of freedom, df = 2,30). The error bars represent the standard deviation of the bootstrapped *F*-statistic distribution and allow comparison between individual bars to assess if one measure is significantly better than the second (e.g., temperature max vs. cannula max) and not if the measures themselves are significant (as both temperature max and cannula max are significant).

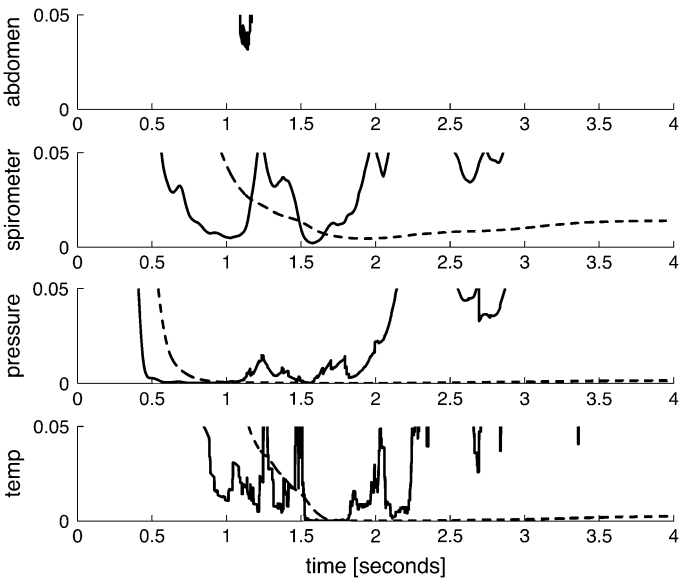

Figure 5 *P* values, as determined by the *F*-statistic, as a function of time for (top to bottom) the abdomen belt, spirometer, pressure, and temperature sensors. Solid lines are for the 10 ms "instantaneous" estimate and dashed lines for the "running" estimate of the *F*-statistic. The abdomen belt showed only a very small window where the instantaneous estimate was significant. Conversely, the spirometer, pressure, and temperature sensors all showed sustained discrimination of the odorant conditions.

In contrast, if one is interested in the temporal dynamics of the sniff, in other words, not only whether odorant-related sniff modulation occurred but also when it first emerged, then the rank ordering of these measurements from most to least time sensitive was as follows: nasal cannula (attached to pressure senor), pneumotachometer flow head (attached to spirometer pressure sensor), and lastly abdominal belt.

It addition to their rank ordering in power and temporal sensitivity, each of these measures enjoys particular advantages and disadvantages that may render them particularly appropriate or inappropriate for a given experiment. Overall, each of the techniques disappoint because they do not directly measure the flow of odorant-laden air that reaches the olfactory sensory surface. Ideally, the "gold-standard" for which we had based our judgments of these 5 external measurement techniques would be a simultaneous recording of the airflow in the upper airway. Because no such device is currently available, we instead judged the techniques on their ability to show odorant-related sniff modulation.

What we measured with the external devices was the rapid change in sniff vigor that was related to the content of the odorant-laden air that reached the olfactory epithelium. Hence, because we did not directly measure the upper airway flow, we did not directly measure the flow that induces the sniff modulation. This sniff modulation manifests as a change in inspiratory drive that is intended to change the amount of odorant-laden air that reaches the sensory surface. The modulation of inspiratory drive changes not just the airflow in the upper airway but also the total air entering the nostril. It is this change in the total air entering the nostril that we measured here. However, in some experiments, particularly those designed to directly study the dynamics of the modulation-inducing airflow, all the techniques used here may be inadequate.

Abdominal respiratory belt

The abdominal respiratory belt was the least powerful of the methods still capable of dissociating odorant-specific sniffing. Respiratory plethysmograph was originally designed as a nonintrusive measure of tidal volume. There are many reports dedicated to assessing this technique's accuracy (Konno and Mead 1967; Milledge and Stott 1977; Chadha et al. 1982; Gonzalez et al. 1984; Watson et al. 1988) and its validity toward diagnosis of respiratory function, especially when using the correlation and phase relationship (the so called Konno–Mead plot) between the abdominal and thoracic expansion (Tripp and Bolton 1998; Willis et al. 2004). That said, all these studies apply to data obtained during "quiet breathing." In contrast, olfactory sniffing constitutes "active breathing" where the normal phase relationship between thoracic and abdominal expansion breaks down. Here we observed that nearly every subject had a different phase relationship between the 2 belts, and even within a single subject, this relationship changed through the course of

the experiment. These disadvantages of using respiratory belts to measure sniffing stem from what is also their major redeeming feature—they do not record from the nose. Thus, one advantage of this method is its applicability to experiments where the nose is engaged within some sort of apparatus that does not permit application of direct measurement devices. A final advantage of this method is its availability. For example, respiratory belts often come "built-in" to MRI scanners and are thus easily applied in fMRI of olfaction experiments. However, the lesson learned from our results is that the belt should be placed at the abdomen and not at the thorax during such experiments.

Temperature sensors

It was surprising to us that the temperature sensor performed so well. Thermistors are a popular technique to measure sniffing (Utenick 1971; Laing 1982, 1983, 1985, 1986; Uchida and Mainen 2003), but they are difficult to calibrate and have poor inherent temporal resolution (temporal resolution can be improved if they are heated above atmospheric temperature, but this can be inconvenient). Indeed, one possible explanation for the marginally higher statistical power of the temperature sensor is the inherent temporal filtering of the device. It is very likely that we could increase the statistical power of the cannula and pneumotachometer by applying a more aggressive low-pass filter. In our analysis, we used a third-order Butterworth low pass with Fc at 10 Hz to prevent altering the temporal dynamics of the measurements. Had we used Fc = 1 Hz or even Fc = 1/3 Hz, it is likely we would have much higher overall discrimination power at the cost of earlier temporal discrimination. On this basis, we repeated our analysis after applying a third-order Butterworth low pass with Fc = 1 Hz. We observed an improvement in the cannula and pneumotachometer *F*-statistic for only the max value summary parameter. We found that the more aggressive low-pass filter "rounded off" the top of each sniff peak, thus making the max value more consistent, yet maintained the overall shape and duration of the sniff, thus not affecting the integral or mean value summary variables.

Finally, despite the statistical power of the temperature sensors, 2 aspects reduce its convenience. First, application of thermistors in demanding environments such as the MRI is restricted. Second, because one nostril can have dramatically lower airflow rates than the other, it is critical to measure using 2 thermistors, one in each nostril, in order to assure sufficient signal.

Pneumotachometer

The pneumotachometer linked to spirometer provided both good statistical power and good temporal resolution. Furthermore, although we used a high-end device, precalibrated USB-based pneumotachometer-spirometer–based instruments are readily available, accurate, and moderately priced. An additional advantage of this method is that the sensor, namely the pneumotachometer, can be linked to the spirometer by pressure tubing alone, with no wires. Considering the availability of pneumotachometers with nylon rather than steel meshes, this allows easy application of the pneumotachometer in demanding environments such as an MRI. In turn, a drawback to pneumotachometers coupled to spirometers is that they require a nasal mask to capture and direct airflow through the device orifice, and breathing through a mask can itself alter breathing patterns (Gilbert et al. 1972; Perez and Tobin 1985; Rodenstein et al. 1985; Paek and McCool 1992). In olfaction experiments, this concern may be unavoidable when a nasal mask is a necessary part of the odorant delivery apparatus. However, if a nasal mask is not necessary for odorant delivery, adding such a mask just for the sake of spirometry is a disadvantage. Finally, an additional concern one may raise regarding the use of a pneumotachometer is that a subject's breathing pattern may be influenced by their awareness of monitoring (Han et al. 1997). However, in our experience, subjects always assume that the nasal mask is only there to deliver odors, and they practically never think that it is also measuring their respiration (Bensafi et al. 2003).

Nasal cannula

The pressure measurement via nasal cannula provided good statistical power and high temporal resolution. Like the pneumotachometer linked to spirometer, the cannula linked to pressure sensor measures differences in pressure resulting from the sniff. However, this device has several advantages over the pneumotachometer. Because it is placed directly in the nares, its temporal resolution is not dampened by the air volume of a nasal mask, as is the case for the pneumotachometer. This is what probably accounts for the slight advantage this method offers in temporal resolution. Furthermore, the geometry of the front end, namely the cannula, enables measurement with or without a nasal mask. Furthermore, like the pneumotachometer and in contrast to thermistors, this method does not entail leading wires into the nose. Use of pressure tubing alone provides maximal flexibility in environments such as the MRI. Last but not least, pressure measurement via nasal cannula is cheap. The cost of the current device was approximately US$120. Indeed, considering these advantages, it is not surprising that this type of method has been applied to devices aimed at measuring sniffing for diagnostic purposes (Frank et al. 2003). The only drawbacks we see to this method are that it is difficult to calibrate and it calls for some care when securing the cannula in place within the nares. Data from 2 subjects were lost in this study due to the cannula slipping out of the nares mid study, albeit these instances were instigated by the numerous other hardware weighing on the cannula tubing. These drawbacks not withstanding, we conclude in recommending pressure measurement via nasal cannula as the best method for measuring sniffing concurrent with olfactory tasks in humans.

Appendix

Pressure sensor diagram

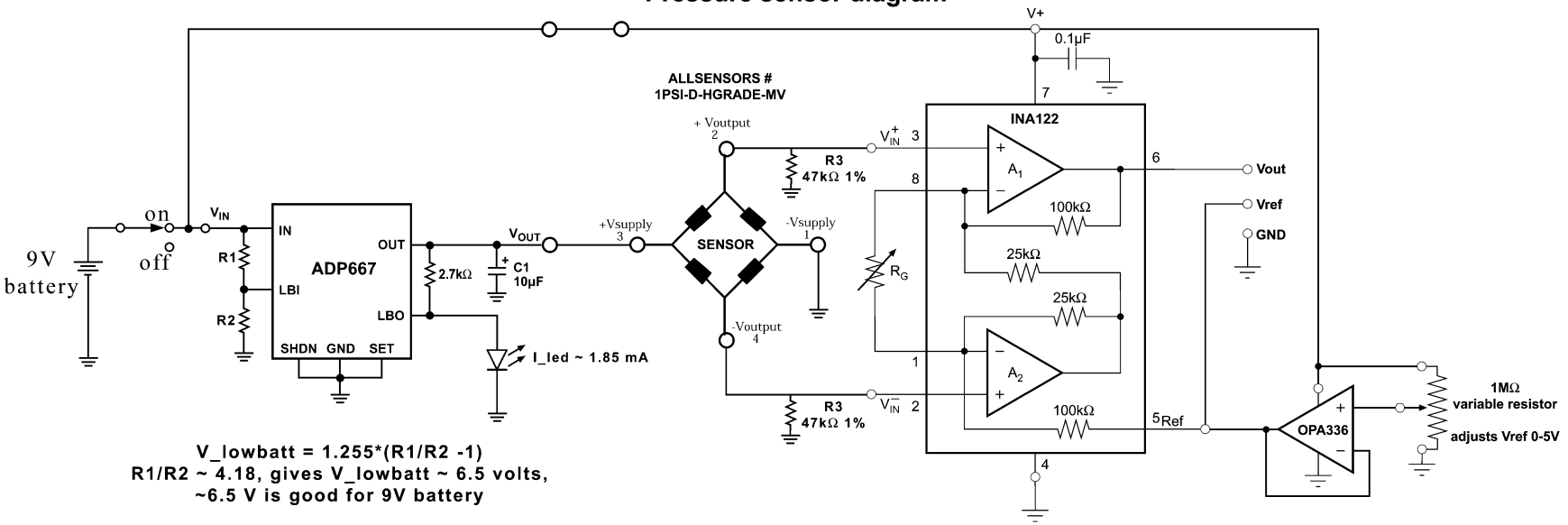

V_lowbatt = 1.255*(R1/R2 -1)
R1/R2 ~ 4.18, gives V_lowbatt ~ 6.5 volts,
~6.5 V is good for 9V battery

choose R1+R2 to minimize load on battery
e.g. R1=910K, R2=220K gives V_lb=6.45V
and I~8 uA

Status LED is the biggest power consumer at ~2mA,
~3X all other components combined.
Eliminating the LED and 2.7kΩ resistor
will dramatically increase battery duration.

$G=5+200k\Omega/R_G$
$Vout=(V^+_{in} - V^-_{in})*G + Vref$

Vout can then be referenced to either Vref or Vgnd
bipolar DAQ system: Vout-Vref=0 at 0 pressure
single-ended DAQ system:Vout-Vgnd=2.5V at 0 pressure

220Ω in series with 200kΩ POT for R_G allows 6<G<914
use series resistor to limit G<1000 to maintain stability

The two R3 resistors are needed to keep the
common-mode input from floating pasted the supply voltage.
Match the two R3 resistors for best CMRR and input offset voltage.

Acknowledgements

This work was supported by a grant from the Army Office of Research 46666-LS. We thank Arak Elite.

References

Allison VC, Katz SH. 1919. An investigation of stenches and odors for industrial purposes. J Ind Eng Chem-Us 11:336–8.

Banzett RB, Mahan ST, Garner DM, Brughera A, Loring SH. 1995. A simple and reliable method to calibrate respiratory magnetometers and respitrace. J Appl Physiol 79:2169–76.

Benignus VA, Prah JD. 1980. A computer-controlled vapor-dilution olfactometer. Behav Res Methods 12:535–40.

Bensafi M, Porter J, Pouliot S, Mainland J, Johnson B, Zelano C, Young N, Bremner E, Aframian D, Khan R, et al. 2003. Olfactomotor activity during imagery mimics that during perception. Nat Neurosci 6:1142–4.

Buonviso N, Amat C, Litaudon P. 2006. Respiratory modulation of olfactory neurons in the rodent brain. Chem Senses 31:145–54.

Chadha TS, Watson H, Birch S, Jenouri GA, Schneider AW, Cohn MA, Sackner MA. 1982. Validation of respiratory inductive plethysmography using different calibration procedures. Am Rev Respir Dis 125:644–9.

Doty RL. 1975. An examination of relationships between the pleasantness, intensity and concentration of 10 odorous stimuli. Percept Psychophysiol 17:492–6.

Efron B, Tibshirani R. 1993. An introduction to the bootstrap. London: Chapman and Hall.

Elsberg CA, Levy I. 1935. The sense of smell. I. A new and simple method of quantative olfactometry. Bull Neurol Inst NY 4:5–19.

Frank RA, Dulay MF, Gesteland RC. 2003. Assessment of the sniff magnitude test as a clinical test of olfactory function. Physiol Behav 78:195–204.

Gamble. 1898. The applicability of Weber's Lab to smell. Am J Psychol 10:82–142.

Gilbert R, Auchincloss JH, Brodsky J, Boden W. 1972. Changes in tidal volume, frequency and ventilation induced by their measurement. J Appl Physiol 33:252–4.

Gonzalez H, Haller B, Watson HL, Sackner MA. 1984. Accuracy of respiratory inductive plethysmograph over wide range of rib cage abdominal compartmental contributions to tidal volume in normal subjects and in patients with chronic obstructive pulmonary disease. Am Rev Respir Dis 130:171–4.

Hahn I, Scherer PW, Mozell MM. 1994. A mass transport model of olfaction. J Theor Biol 167:115–28.

Han JN, Stegen K, Cauberghs M, Van de Woestijne KP. 1997. Influence of awareness of the recording of breathing on respiratory pattern in healthy humans. Eur Respir J 10:161–6.

Hasegawa M, Kern EB. 1977. The human nasal cycle. Mayo Clin Proc 52: 28–34.

Johnson BN, Mainland JD, Sobel N. (2003). Rapid olfactory processing implicates subcortical control of an olfactomotor system. J Neurophysiol 90:1084–94.

Johnston JW. 1967. Quantification of olfactory stimuli. In: Brown CC, editor. Methods in psychophysiology. Baltimore, MD: The Williams & Wilkins Company.

Kepecs A, Uchida N, Mainen ZF. 2006. The sniff as a unit of olfactory processing. Chem Senses 31:167–79.

Keyhani K, Scherer PW, Mozell MM. 1995. Numerical simulation of airflow in the human nasal cavity. J Biomech Eng 117:429–41.

Kobal G. 1985. Pain-related electrical potentials of the human nasal mucosa elicited by chemical stimulation. Pain 22:151–63.

Konno K, Mead J. 1967. Measurement of separate volume changes of rib cage and abdomen during breathing. J Appl Physiol 22:407–22.

Laing DG. 1982. Characterisation of human behaviour during odour perception. Perception 11:221–3.

Laing DG. 1983. Natural sniffing gives optimum odour perception for humans. Perception 12:99–117.

Laing DG. 1985. Optimum perception of odor intensity by humans. Physiol Behav 34:569–74.

Laing DG. 1986. Identification of single dissimilar odors is achieved by humans with a single sniff. Physiol Behav 37:163–70.

Laurent G. 2002. Olfactory network dynamics and the coding of multidimensional signals. Nat Rev Neurosci 11:884–95.

Le Magnen J. 1945. Etude des facteurs dynamiques de l'excitation olfactive. L'Année Psychologique 6:77–89.

Mainland J, Sobel N. 2006. The sniff is part of the olfactory percept. Chem Senses 31:181–96.

Milledge J, Stott F. 1977. Inductive plethysmograph—a new respiratory transducer. J Physiol 267:4–5.

Paek D, McCool FD. 1992. Breathing patterns during varied activities. J Appl Physiol 73:887–93.

Paulsen E. 1882. Experimentelle untersuchungen uber Stromungen der Luft in der Nasenhohle. Sitzungsber Akad Wiss.

Perez W, Tobin MJ. 1985. Separation of factors responsible for change in breathing pattern induced by instrumentation. J Appl Physiol 59: 1515–20.

Prah D, Sears S, Walker JC. 1995. Modern approaches to air dilution olfactometry. In: Doty RL, editor. Handbook of olfaction and gustation. New York: Marcel Dekker, Inc. p 227–57.

Principato JJ, Ozenberger JM. 1970. Cyclical changes in nasal resistance. Arch Otolaryngol 91:71–7.

Rodenstein DO, Mercenier C, Stanescu DC. 1985. Influence of the respiratory route on the resting breathing pattern in humans. Am Rev Respir Dis 131:163–66.

Schoenfeld TA, Cleland TA. 2006. Anatomical contributions to odorant sampling and representation in rodents: zoning in on sniffing behavior. Chem Senses 31:131–44.

Sobel N, Prabhakaran V, Desmond JE, Glover GH, Goode RL, Sullivan EV, Gabrieli JD. 1998. Sniffing and smelling: separate subsystems in the human olfactory cortex. Nature 392:282–6.

Sobel N, Thomason ME, Stappen I, Tanner CM, Tetrud JW, Bower JM, Sullivan EV, Gabrieli JD. 2001. An impairment in sniffing contributes to the olfactory impairment in Parkinson's disease. Proc Natl Acad Sci USA 98: 4154–9.

Spors H, Grinvald A. 2002. Spatio-temporal dynamics of odor representations in the mammalian olfactory bulb. Neuron 34:301–15.

Tripp H, Bolton J. 1998. Phrenic nerve injury following cardiac surgery: a review. J Cardiothorac Surg 31:1265–7.

Tucker D. 1963. Physical variables in the olfactory stimulation process. Gen Physiol 46:453–89.

Uchida N, Mainen ZF. 2003. Speed and accuracy of olfactory discrimination in the rat. Nat Neurosci 6:1224–9.

Utenick MR. 1971. Design of a hot-wire anemometer. ISA Trans 10: 21–8.

Walker JC, Kendal-Reed M, Hall SB, Morgan WT, Polyakov VV, Lutz RW. 2001. Human responses to propionic acid. II. Quantification of breathing responses and their relationship to perception. Chem Senses 26:351–8.

Warren DW, Walker JC, Drake AF, Lutz RW. 1994. Effects of odorants and irritants on respiratory behavior. Laryngoscope 104:623–6.

Watson HL, Poole DA, Sackner MA. 1988. Accuracy of respiratory inductive plethysmographic cross-sectional areas. J Appl Physiol 65: 306–8.

Willis BC, Graham AS, Wetzel R, Newth CJL. 2004. Respiratory inductance plethysmography used to diagnose bilateral diaphragmatic paralysis: a case report. Pediatr Crit Care Med 5:399–402.

Youngentob SL, Mozell MM, Sheehe PR, Hornung DE. 1987. A quantitative analysis of sniffing strategies in rats performing odor detection tasks. Physiol Behav 41:59–69.

Zhao K, Dalton P, Yang GC, Scherer PW. 2006. Numerical modeling of turbulent and laminar airflow and odorant transport during sniffing in the human and rat nose. Chem Senses 31:107–18.

Zhao K, Scherer PW, Hajiloo SA, Dalton P. 2004. Effect of anatomy on human nasal air flow and odorant transport patterns: implications for olfaction. Chem Senses 29:365–79.

Accepted July 24, 2006